AIP | Applied Physics Letters

Temperature dependence of frequency response characteristics in organic field-effect transistors

Xubing Lu, Takeo Minari, Chuan Liu, Akichika Kumatani, J.-M. Liu et al.

Citation: Appl. Phys. Lett. **100**, 183308 (2012); doi: 10.1063/1.4711211
View online: http://dx.doi.org/10.1063/1.4711211
View Table of Contents: http://apl.aip.org/resource/1/APPLAB/v100/i18
Published by the American Institute of Physics.

Temperature dependence of frequency response characteristics in organic field-effect transistors

Xubing Lu,[1,2] Takeo Minari,[2,3,a)] Chuan Liu,[2] Akichika Kumatani,[2] J.-M. Liu,[1,4] and Kazuhito Tsukagoshi[2,5,a)]
[1]*Institute for Advanced Materials, School of Physics and Telecommunication, South China Normal University, Guangzhou 510006, China*
[2]*International Center for Materials Nanoarchitectonics (WPI-MANA), National Institute for Materials Science (NIMS), Tsukuba, Ibaraki 305-0044, Japan*
[3]*RIKEN, Wako, Saitama 305-0044, Japan*
[4]*National Laboratory of Solid State Microstructures, Nanjing University, Nanjing 210093, China*
[5]*Core Research for Evolutional Science & Technology (CREST), Japan Science and Technology Agency (JST), Kawaguchi, Saitama 332-0012, Japan*

(Received 22 February 2012; accepted 15 April 2012; published online 4 May 2012)

The frequency response characteristics of semiconductor devices play an essential role in the high-speed operation of electronic devices. We investigated the temperature dependence of dynamic characteristics in pentacene-based organic field-effect transistors and metal-insulator-semiconductor capacitors. As the temperature decreased, the capacitance-voltage characteristics showed large frequency dispersion and a negative shift in the flat-band voltage at high frequencies. The cutoff frequency shows Arrhenius-type temperature dependence with different activation energy values for various gate voltages. These phenomena demonstrate the effects of charge trapping on the frequency response characteristics, since decreased mobility prevents a fast charge response for alternating current signals at low temperatures. © *2012 American Institute of Physics*. [http://dx.doi.org/10.1063/1.4711211]

In recent decades, extensive research has been conducted on organic field-effect transistors (OFETs) due to their attractive features such as low cost, large area, and flexibility.[1–4] Most of the work so far has dealt with their static direct current (DC) characteristics such as output and transfer characteristics, through which some of the basic device parameters such as field-effect mobility (μ_{FET}), threshold voltage (V_T), and subthreshold swing (S) are extracted. Temperature dependence of these parameters has provided much insight with regard to the operation mechanisms of OFETs, particularly on charge transport in organic semiconductors.[5,6] On the other hand, with the increasing use of organic electronic devices in practical applications,[7] improvement in the frequency response characteristics (FRC) of OFETs becomes an essential requirement for high-speed operation of these devices.[8–13] For instance, the frequency of 13.56 MHz is normally used for RF-ID tags, considered to be one possible application for organic devices.[14] The dynamic alternating current (AC) characteristics can also provide fundamental information on charge transport in semiconductors and its limiting factors such as charge trapping at the semiconductor/dielectric interface.[15–18] In the past, some works have been done to demonstrate the FRC of OFETs and different factors responsible for their FRC, such as channel length,[8,19] parasitic capacitance,[20] and contact resistance[19] were proposed. However, most of these woks have been done through room temperature measurements, although temperature dependence of FRC is expected to provide tremendous information about the important factors of AC characteristics such as an effect of charge transport on the dynamic characteristics.

In this study, the temperature dependence of FRC was demonstrated on metal-insulator-semiconductor (MIS) capacitors and OFETs using pentacene as a *p*-type semiconductor. We carried out capacitance-voltage (*C-V*) and capacitance-frequency (*C-f*) measurements at various temperatures to investigate the dominant factors that affect FRC of organic devices. In particular, we focused on two device parameters, flat band voltage (V_{FB}) and cutoff frequency (f_c), and the dependence of these two parameters on the gate voltage (V_G), temperature, and the applied frequency was examined. Through the systematic measurements, strong temperature and frequency dependence of the $V_{FB,}$ and temperature and V_G dependence of f_c were observed. The mechanism of these tendencies is discussed with correlation to static measurement results, and charge trapping in organic semiconductor was found to be critical for AC characteristics.

In experiments, pentacene-based OFETs and MIS capacitors were fabricated on the same substrate by the following procedures. A highly doped Si (100) wafer with a 50 nm thick thermally oxidized SiO_2 layer was used as a substrate, where the Si wafer is used as the gate electrode and the SiO_2 layer acts as a gate insulator. The surface was ultrasonically cleaned in acetone and 2-propanol, followed by UV-O_3 treatment for 5 min. To improve the interfacial quality between the gate insulator and organic semiconductor layer, one layer of polystyrene (PS) with ~30 nm thickness was deposited by spin-coating. The PS layer was annealed in air for 5 min at 120 °C. Pentacene (Aldrich, purified with temperature gradient sublimation) was vacuum-deposited onto the PS layer-covered SiO_2 surface at a growth rate of 0.1 nm/s up to a thickness of 40 nm. The pentacene

[a)]Authors to whom correspondence should be addressed. Electronic addresses: minari.takeo@nims.go.jp and tsukagoshi.kazuhito@nims.go.jp.

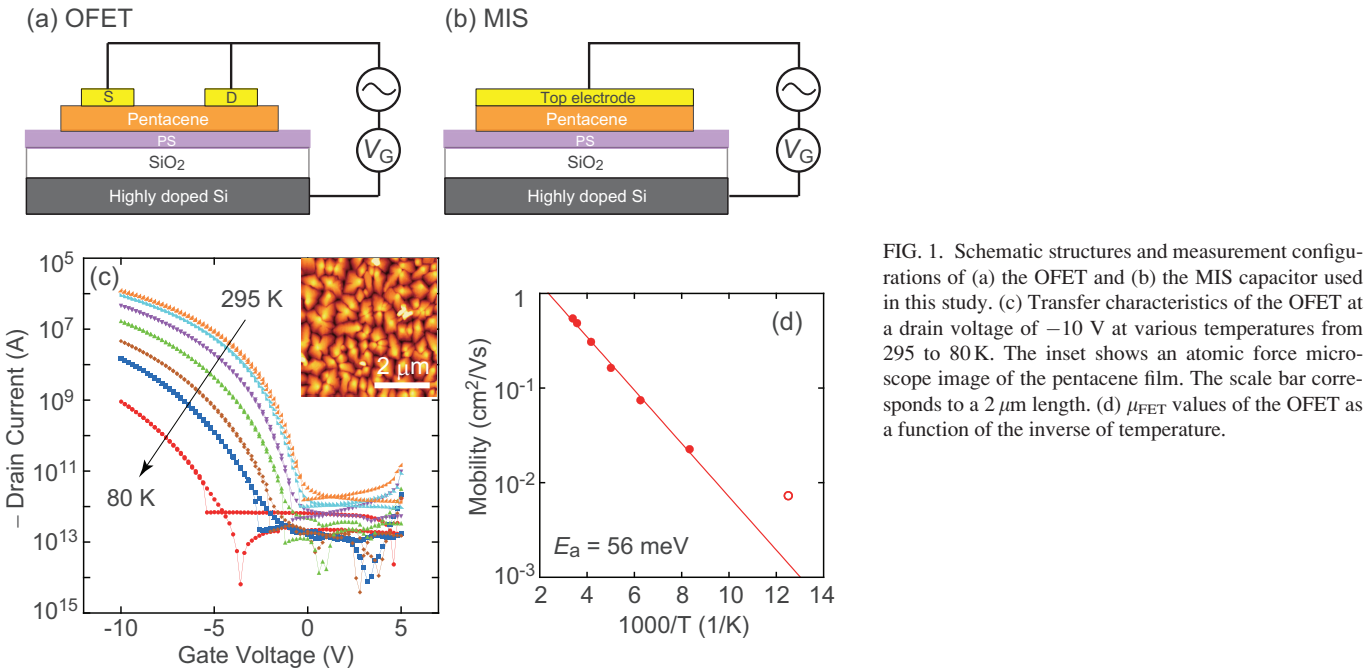

FIG. 1. Schematic structures and measurement configurations of (a) the OFET and (b) the MIS capacitor used in this study. (c) Transfer characteristics of the OFET at a drain voltage of −10 V at various temperatures from 295 to 80 K. The inset shows an atomic force microscope image of the pentacene film. The scale bar corresponds to a 2 μm length. (d) μ_{FET} values of the OFET as a function of the inverse of temperature.

deposition was carried out through a metal mask to isolate the active area of each device. Finally, copper (Cu) electrodes were deposited by vacuum evaporation through a metal mask and thus the OFETs and MIS capacitors were formed on the same substrate. Schematic cross-sections of these devices are shown in Figs. 1(a) and 1(b). An atomic force microscope image of the pentacene surface is shown in the inset of Fig. 1(c). The AC characteristics of the MIS capacitor were measured by an *LCR* meter (Agilent E4980A) and the static DC characteristics of the transistors were measured using an Agilent 4156C semiconductor device analyzer. All electrical measurements were performed under dark in high vacuum ($<5 \times 10^{-3}$ Pa). The *C-V* characteristics were measured by applying a DC voltage in the range of 10 to −10 V along with a probe AC voltage of 100 mV. The *C-f* characteristics were obtained by sweeping the frequency with a fixed V_G.

We first examined the static DC characteristics of the pentacene-based OFETs at various temperatures. The measured OFET had a channel length (L) and width (W) of 100 μm and 750 μm, respectively. Figure 1(c) represents the transfer characteristics of the OFET at a drain voltage of −10 V at various temperatures from 295 K to 80 K. One can observe a decrease in the drain current and a negative shift in the turn-on voltage with lowering of the temperature. These tendencies indicate thermally activated charge transport, which agrees well with the previously reported trends for OFETs with a polycrystalline or amorphous semiconductor film.[21–23] The field-effect mobility (μ_{FET}) was determined to be 0.58 cm^2/V s at 295 K. An Arrhenius plot of the μ_{FET} is shown in Fig. 1(d), and the activation energy (E_a) was determined to be 56 meV. This value also corresponds well with previously reported E_a values for OFETs based on a polycrystalline pentacene film.[24]

The *C-V* characteristics of the MIS capacitor were measured under various frequencies from 100 Hz to 100 kHz at different temperatures. Figures 2(a) and 2(b) show the characteristics obtained at 295 K and 120 K, respectively. In the case of *p*-type organic semiconductor devices, charge carriers were injected into the semiconductor layer from the upper electrode when a negative V_G was applied, and these accumulated at the semiconductor/insulator interface. In the figures, the *C-V* curves exhibit a typical output from accumulation to depletion when the voltage sweeps from −10 V to +10 V. The most important feature observed in the present *C-V* curves is the large dispersion in the capacitance for varying frequencies and a shift in V_{FB} observed at low temperatures. At a temperature of 295 K, the maximum capacitance (C_{max}) was obtained at high negative V_G, indicating the formation of a charge accumulation layer at the insulator/organic semiconductor interface and C_{max} corresponds to the

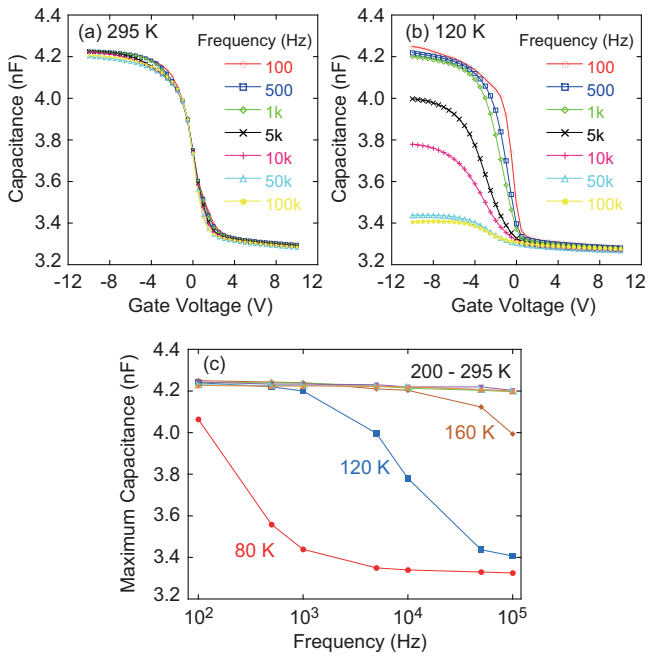

FIG. 2. (a) *C-V* characteristics of the MIS capacitor obtained at (a) 295 K and (b) 120 K at various frequencies. (c) The maximum capacitance of the MIS capacitor as a function of frequency for different temperatures.

capacitance of the gate insulator. The *C-V* characteristics of the MIS capacitor for various frequencies are fully overlapped at 295 K, and almost no capacitance-voltage frequency dispersion (CVFD) was observed in the temperature range down to 200 K. The C_{max} started to decrease at high frequencies and the *C-V* characteristics tended to show CVFD when the temperature was down to 160 K or lower (Fig. 2(b)). Significantly large CVFD was observed at a temperature of 80 K (not shown). The change in the C_{max} as a function of frequency at various temperatures is summarized in Fig. 2(c). The dependence of C_{max} on temperature and frequency can be understood by the thermally activated charge transport and charge response for the AC signal in the semiconductor layer. With lowering of the temperature, the charge mobility decreases due to charge trapping in the pentacene film, as seen in the temperature dependence of μ_{FET} in Fig. 1(d). The lower mobility prevents charges from responding to AC signals at low temperatures. Thus, the semiconductor layer acts as a dielectric for the AC signals at higher frequencies, which decreases C_{max}. This tendency is clearly observed at a temperature of 80 K, where C_{max} has almost the same value as the minimum depletion mode capacitance (C_{min}) of 3.3 nF at high frequencies (Fig. 2(c)), indicating that the semiconductor layer is fully depleted for the probe signals.

In silicon-based devices, extensive studies have been carried out on the V_{FB} of MIS structures, which directly affects the V_T of transistors, particularly for high-*k* gate dielectric devices.[24,25] We extracted the V_{FB} values from the *C-V* curves of the pentacene-based MIS capacitor at various temperatures by using an experienced method derived by the Motorola Digital DNA laboratory as the voltage corresponding to $C_{FB} = (C_{max} - C_{min}) \times 0.66 + C_{min}$, where C_{FB} is the flat-band capacitance.[26] The frequency dependence of V_{FB} is summarized in Fig. 3. Similar to C_{max}, the V_{FB} is found to be dependent on applied frequency and temperature. The V_{FB} is almost constant for a temperature at 280 K, but varies from −0.5 V at 100 Hz to −2.8 V at 100 kHz at a temperature of 160 K, and an even larger shift was observed at lower temperatures. This large shift in V_{FB} may greatly change the V_T value of the corresponding OFET devices when they operate under various frequency situations, which would lead to the unstable device properties. To realize V_T stability under high-frequency operation of OFETs, it is critical to understand the mechanism of this V_{FB} frequency dispersion.

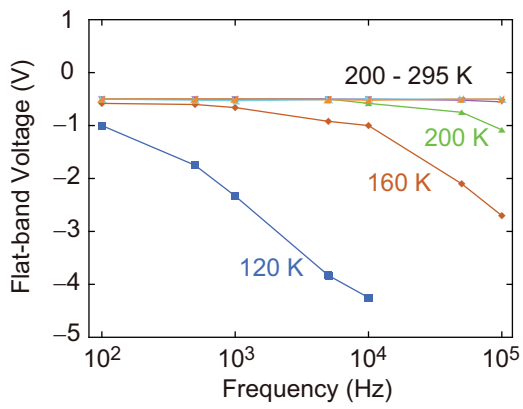

FIG. 3. Flat-band voltage of the MIS capacitor as a function of frequency obtained at different temperatures.

It is known that the V_{FB} can be determined by the metal-semiconductor work function difference ϕ_{MS} and various fixed or trapped charges in MIS capacitors, as described by the following expression:[27]

$$V_{FB} = \phi_{MS} - \frac{Q_f}{C_{ins}} - \frac{Q_{it}(\phi_s)}{C_{ins}} - \frac{1}{C_{ins}}\int_0^{t_{ins}} \frac{x}{t_{ins}}\rho_s(x)dx - \frac{1}{C_{ins}}\int_0^{t_{ins}} \frac{x}{t_{ins}}\rho_m(x)dx, \quad (1)$$

where Q_f is the fixed charge located near the semiconductor/insulator interface and Q_{it} is the interface trapped charge (occupation of interface trap states is a function of surface potential ϕ_S). ρ_s and ρ_m are the insulator charges and mobile ions per unit volume, and C_{ins} and t_{ins} are the insulator capacitance and thickness, respectively. In the case of organic thin-film devices, the effect of charge traps associated with the organic semiconductor layer seems to be more significant than that of other fixed charges such as dielectric trapped charges and mobile ions. Thus, we consider that Q_{it} (ϕ_S) is probably a dominant factor that mainly affects V_{FB}. It should be noted that charge trapping at the interface between the top electrode and the organic semiconductor also causes a large V_{FB} shift in the case of organic thin-film devices. The effect of the top electrode interface on V_{FB} can be found in our previous report, where the insertion of an injection-assist layer into the contact interface causes a large positive shift in the *C-V* characteristics.[28] Since charge trapping at both semiconductor/insulator and electrode/semiconductor interfaces should be a thermally activated process, it can be concluded that the V_{FB} can be temperature dependent.

The above results demonstrate that charge trapping in an organic semiconductor layer plays an important role in the V_{FB} frequency response characteristics. To further investigate the frequency response characteristics of OFETs, we carried out *C-f* measurements on OFETs at various temperatures for extraction of f_c, the most common parameter showing the dynamic response capability of OFETs. f_c can be defined as[8,19]

$$f_c = \frac{1}{2\pi} \cdot \frac{g_m}{C_{ins}WL} = \frac{\mu(V_G - V_T)}{2\pi L^2}, \quad (2)$$

where g_m is the transconductance. As seen in Eq. (2), f_c should be a function of V_G and L, which has already been clarified for OFET devices.[19] The *C-f* measurement configuration used in the present study is shown in Fig. 1(a), where source and drain electrodes are electrically shorted and connected to the *LCR* meter, as described in Ref. 19. The OFET has comb-shaped source/drain electrodes with $L = 150\,\mu m$. The obtained *C-f* characteristics at a constant V_G of −20 V at different temperatures are shown in Fig. 4(a); here, the *C-f* characteristics obviously depend on the measurement temperature. The f_c values were estimated as the intersection points of the extrapolated fitting lines and the capacitance of the low frequency region (Fig. 4(a)). The extracted f_c values are plotted as a function of the inverse of the temperature with least square fitting lines at various V_Gs in Fig. 4(b). In this figure, it can be clearly seen that the f_c values show Arrhenius-type temperature dependence as observed for μ_{FET} of the OFET in Fig. 1(d). At higher V_G, the

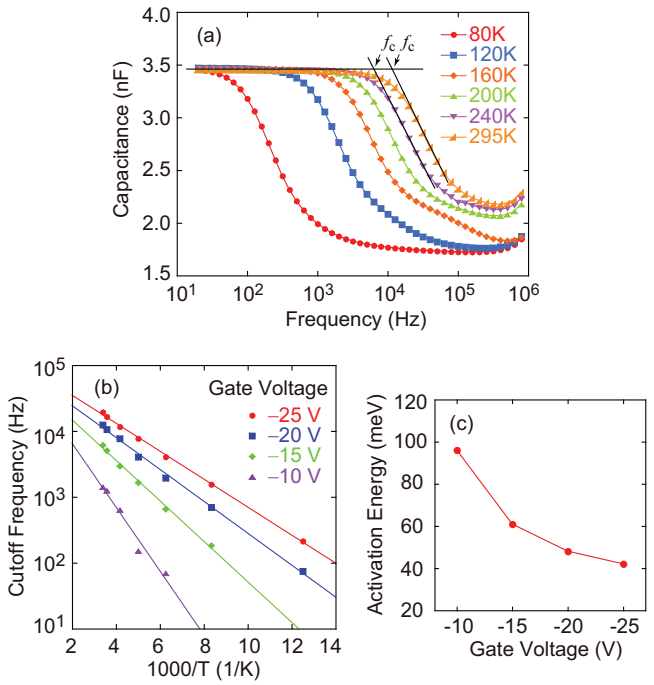

FIG. 4. (a) *C-f* characteristics of the OFET at a gate voltage of −20 V at various temperatures. (b) Cutoff frequency of the OFET as a function of the inverse of temperature for various gate voltages. (c) Activation energy of the OFET as a function of gate voltage.

f_c values become higher and the slope of the fitting line is smaller (Fig. 4(b)). Accordingly, E_a values of f_c at different V_Gs were calculated and are summarized as a function of V_G in Fig. 4(c). These values are very similar to the E_a of 56 meV obtained from μ_{FET} in Fig. 1(d), indicating strong correlation between f_c and μ_{FET}. The observed temperature and V_G dependence of f_c is related to multiple trapping and release model for charge transport.[22] In this model, charge transport occurs in the extended state and interacts with shallow charge trap states localized in the forbidden band. Increased charge density due to an increase in V_G fills localized trap states and reduces trap distribution in the organic semiconductor, which decreases activation energy for charge transport. This mechanism results in the temperature and V_G dependence of the mobility, which can be associated with f_c as indicated in Eq. (2). Thus, thermally activated charge transport caused by charge trapping at localized states is a critical factor that limits frequency response characteristics of OFETs.

In summary, the frequency response characteristics of pentacene-based OFETs and MIS capacitors, particularly instability of V_{FB} and f_c, are investigated through temperature dependent *C-V* and *C-f* measurements. At low temperature, the *C-V* characteristics tend to show large frequency dispersion and V_{FB} is shifted to a negative voltage. A significant temperature dependence is also observed for the *C-f* characteristics, where the f_c shows Arrhenius-type temperature dependence with different E_a for variation of V_G. These phenomena can be explained by thermally activated charge transport described by a multiple trapping and release model, as decreased charge carrier mobility prevents fast charge response for AC signals at low temperatures.

The authors would like to thank Dr. T. Miyadera (JST-PREST) for valuable discussions. This study was partially supported by a Grant for Advanced Industrial Technology Development (No. 11B11016d) from the New Energy and Industrial Technology Development Organization (NEDO), Japan. It was also supported in part by a Grant-in-Aid for Scientific Research (No. 218505) from the Ministry of Education, Culture, Sport, Science, and Technology of Japan.

[1]C. D. Dimitrakopoulos and P. R. L. Malenfant, Adv. Mater. **14**, 99 (2002).
[2]H. E. Katz, Chem. Mater. **16**, 4748 (2004).
[3]M. Kitamura and Y. Arakawa, J. Phys.: Condens. Matter. **20**, 184011 (2008).
[4]Y. Yang and F. Wudl, Adv. Mater. **21**, 1401 (2009).
[5]S. F. Nelson, Y.-Y. Lin, D. J. Gundlach, and T. N. Jackson, Appl. Phys. Lett. **72**, 1854 (1998).
[6]T. Minari, T. Nemoto, and S. Isoda, J. Appl. Phys. **96**, 769 (2004).
[7]K. Sanderson, Nature (London) **445**,473 (2007).
[8]S. Scheinert and G. Paasch, Phys. Status Solidi A **201**, 1263 (2004).
[9]Y. Y. Noh, N. Zhao, M. Caironi, and H. Sirringhaus, Nat. Nanotechnol. **2**, 784 (2007).
[10]T. Sekitani, Y. Noguchi, U. Zschieschang, H. Klauk, and T. Someya, Proc. Natl. Acad. Sci. U.S.A. **105**, 4976 (2009).
[11]D. Bode, K. Myny, B. Verreet, B. van der Putten, P. Bakalov, S. Steudel, S. Smout, P. Vicca, J. Genoe, and P. Heremans, Appl. Phys. Lett. **96**, 133307 (2010).
[12]U. Palfinger, C. Auner, H. Gold, A. Haase, J. Kraxner, T. Haber, M. Sezen, W. Grogger, G. Domann, G. Jakopic, J. Krenn, and B. Stadlober, Adv. Mater. **22**, 5115 (2010).
[13]T. Miyadera, M. Nakayama, and K. Saiki, Appl. Phys. Lett. **89**, 172117 (2006).
[14]R. Rotzoll, S. Mohapatra, V. Olariu, R. Wenz, M. Grigas, K. Dimmler, O. Shchekin, and A. Dodabalapur, Appl. Phys. Lett. **88**, 123502 (2006).
[15]I. Torres, D. M. Taylor, and E. Ito, Appl. Phys. Lett. **85**, 314 (2004).
[16]A. Wang, I. Kymissis, V. Bulović, and A. I. Akinwande, Appl. Phys. Lett. **89**, 112109 (2006).
[17]T. Miyadera, M. Nakayama, and K. Saiki, Appl. Phys. Lett. **89**, 172117 (2006).
[18]X. B. Lu, T. Minari, A. Kumatani, C. Liu, and K. Tsukagoshi, Appl. Phys. Lett. **98**, 243301 (2011).
[19]T. Miyadera, T. Minari, K. Tsukagoshi, H. Ito, and Y. Aoyagi, Appl. Phys. Lett. **91**, 013512 (2007).
[20]M. Caironi, Y. Y. Noh, and H. Sirringhaus, Semicond. Sci. Technol. **26**, 034006 (2011).
[21]Y. Y. Lin, D. J. Gundlach, and T. N. Jackson, Appl. Phys. Lett. **72**, 1854 (1998).
[22]G. Horowitz, M. E. Hajlaoui, and R. Hajlaoui, J. Appl. Phys. **87**, 4456 (2000).
[23]T. Minari, T. Nemoto, and S. Isoda, J. Appl. Phys. **99**, 034506 (2006).
[24]K. Kakushima, K. Okamoto, M. Adachi, K. Tachi, P. Ahmet, K. Tsutsui, N. Sugii, T. Hattori, and H. Iwai, Solid-State Electron. **52**, 1280 (2008).
[25]W. Wang, K. Akiyama, W. Mizubayashi, T. Nabatame, H. Ota, and A. Toriumi, J. Appl. Phys. **105**, 064108 (2009).
[26]M. Zhu, J. Zhu, J. M. Liu, and Z. G. Liu, Appl. Phys. A **80**, 135 (2005).
[27]D. K. Schroder, *Semiconductor Material and Device Characterization* (Wiley, New York, 2006).
[28]P. Darmawan, T. Minari, A. Kumatani, Y. Li, C. Liu, and K. Tsukagoshi, Appl. Phys. Lett. **100**, 013303 (2012).